

Prediction of chloride diffusion coefficient of concrete under flexural cyclic load

Tran Van Mien¹, Boonchai Stitmannathum*² and Toyoharu Nawa³

¹Faculty of Civil Engineering, HoChiMinh City University of Technology, HCMC, Vietnam

²Department of Civil Engineering, Chulalongkorn University, BKK, Thailand

³Graduate School of Engineering, Hokkaido University, Hokkaido, Japan

(Received October 16, 2009, Accepted November 4, 2010)

Abstract. This paper presented the model to predict the chloride diffusion coefficient in tension zone of plain concrete under flexural cyclic load. The fictitious crack based analytical model was used together with the stress degradation law in cracked zone to predict crack growth of plain concrete beams under flexural cyclic load. Then, under cyclic load, the chloride diffusion, in the steady state and one dimensional regime, through the tension zone of the plain concrete beam, in which microcracks were formed by a large number of cycles, was simulated with assumptions of continuously straight crack and uniform-size crack. The numerical analysis in terms of the chloride diffusion coefficient, D_{10b} normalized D_{10b} , crack width and crack length was issued as a function of the load cycle, N , and load level, SR . The nonlinear model as regarding with the chloride diffusion coefficient in tension zone and the load level was proposed. According to this model, the chloride diffusion increases with increasing load level. The predictions using model fit well with experimental data when we adopted suitable crack density and tortuosity parameter.

Keywords: model; chloride diffusion coefficient; flexural cyclic load; crack growth.

1. Introduction

In marine environment, the chloride induced corrosion of reinforcement is one of the major deteriorations of reinforced concrete structures. By the time, chloride ions penetrate from the concrete surface and reach the embedded steel, and chloride ions make the embedded steels corrode. The chloride penetration into concrete is a complex phenomenon depending on the material characteristics of concrete, the environmental conditions and the service loads during the service life time (Tran *et al.* 2009 and Yoon 2009). Generally, concrete is dense and water tight material in uncracked stage. Unfortunately, at field, concrete structures usually reveal cracks due to shrinkage, placing and consolidations, and imposed loads (Gérard and Marchand 2000 and Tran *et al.* 2009). Bridges and highway pavements, where millions of cycles of loads are applied during their service lives, show internal cracks inside the concrete cover. These cracks widen or become connected as the number of load cycle increases (Gontar *et al.* 2000). The cracks formed due to cyclic load can increase the chloride diffusion coefficients of concretes. Consequently, the chloride penetration into concrete structures in the marine environment is accelerated, when cyclic loads are applied to them.

There have been many models developed either to predict the chloride diffusion into plain

* Corresponding author, Professor, E-mail: fcebst@eng.chula.ac.th

concrete in the uncracked stages, without loading stage, or to simulate deformation of plain concrete, in terms of crack width and crack length, in the imposed load stage (Tran *et al.* 2009, Zhang *et al.* 1999 and Ulfkjær *et al.* 1995). However, under cyclic loads, there are no models to be able to predict both fatigue deformations and the chloride penetration under fatigue. This paper describes the crack growth of plain concrete beam under flexural cyclic load. Assume that crack network is continuous, the size of crack is uniform and crack length at the bottom side of concrete beam is equal to that of the edge side, then effects of flexural cyclic load on the chloride diffusion coefficient in the tension zone of plain concrete beams at one dimensional regime are proposed. The fictitious crack based analytical model is used to predict crack growth in plain concrete beams under flexural cyclic load, and the stress degradation law is applied in the developing stage of the fictitious crack. The models of crack length or crack width, the chloride diffusion coefficients those vary by load level, SR , and the number of cycles, N , are verified as compared with experimental results.

2. Simulation of crack growth of plain concrete beam under flexural cyclic load

The crack growth process of plain concrete beam with depth h , width B and span l under flexural cyclic load can be generally divided into two stages: the fictitious crack initiation stage and the fictitious crack developing stage. The former will occur when bending load reaches the first crack load. In the later, as shown in Fig. 1 stress distribution is nonlinear and linear in the cracked zone and uncracked zone, respectively (Zhang *et al.* 1999).

In the cracked zone, a linear crack opening profile can be expressed

$$w = \delta \left(1 - \frac{x}{ah}\right) \quad (1)$$

where w is the crack width at a specific location x , and δ is crack mouth opening.

The stress distribution in the cracked zone, $\sigma_I(x)$, can be expressed as a function of crack length ah , $0 \leq a \leq 1$, and δ , combining stress-crack relationship and Eq. (1) as below (Zhang *et al.* 1999 and Tada 1985)

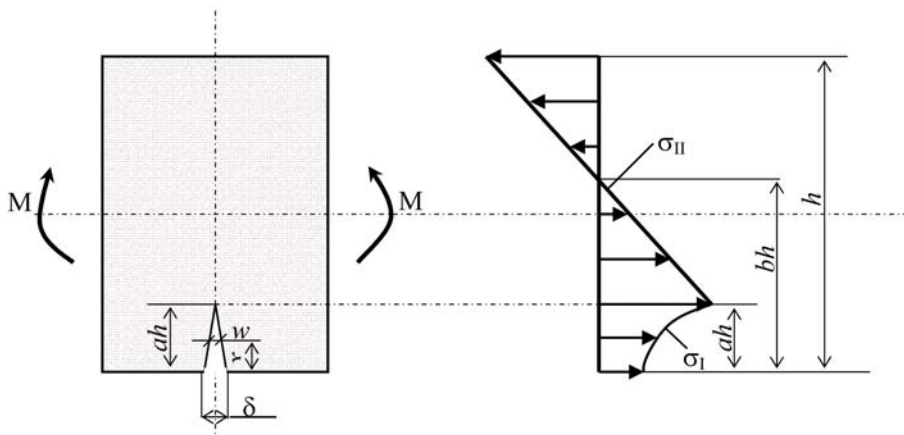


Fig. 1 Distribution of stress in the second stage

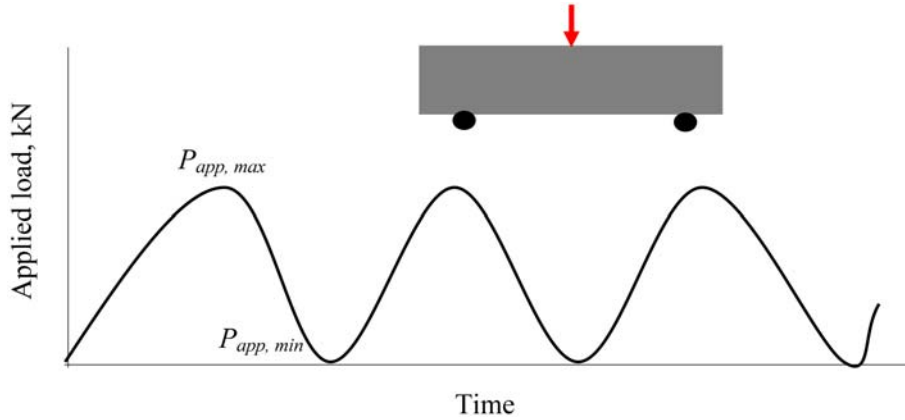


Fig. 2 Load procedure in flexural cyclic test

$$\sigma_I(x) = \sigma(w) = \sigma\left(\delta\left(1 - \frac{x}{ah}\right)\right) \quad (2)$$

For flexural cyclic load, in the cracked zone, $\sigma_I(x)$ can be contributed by stress degradation law. With plain concrete beam, the stress degradation law can be expressed as a function of logarithm of the number of cycles

$$\frac{\sigma_N}{\sigma_1} = 1 - \phi k \log(N) \quad (3)$$

where σ_N and σ_1 are the stresses in the cracked zone at the at maximum applied load, $P_{app, max}$, after N cycles and the first cycle, respectively. ϕ presents the influence of minimum crack width formed at the minimum applied load, $P_{app, min}$, on the stress degradation. When $P_{app, min}$ equals to zero, the maximum degradation, $\phi = 1$, will occur. On the contrary, the minimum degradation, $\phi = 0$, will appear when the crack width formed by $P_{app, min}$ equals to that formed by $P_{app, max}$. In this research, plain concrete was used, and $P_{app, min}$ was equal to zero (Fig. 2). Hence, the maximum degradation will occur, $\phi = 1$.

For plain concrete, k is expressed depending on $w_{1,N}$ and ϕ as

$$k = \phi(0.08 + 4w_{1,N}) \quad (4)$$

where $w_{1,N}$ is the crack width, in the cracked zone, formed by $P_{app, max}$ at the cycle N . From Eqs. (3) and (4), we see that when the number of cycles increases, $w_{1,N}$ increases and consequently the stress in the cracked zone reduces until σ_N equals to zero, at which fracture of concrete beam occurs.

Based on the experimental data, Zhang *et al.* (1999) proposed that σ_1 can be related to tensile strength of concrete, σ_t , and initially ramped up crack width w_i where the bending load is ramped up to $P_{app, max}$, as below

$$\frac{\sigma_1}{\sigma_t} = c + dw_i \quad (5)$$

where c and d are parameters depending on w_i as shown in Table 1.

Assumed that the stress distribution in the uncracked zone, $\sigma_{II}(x)$, is linear, $\sigma_{II}(x)$ can be related to

Table 1 Parameters of plain concrete

Material	w_i (mm)	c (1/mm)	d (1/mm)
Plain concrete	0-0.04	1	-33.48
	0.04-0.18	0.569	-8.12
	0.18-0.75	0.321	-2.49
	0.75-2	0.187	-0.84

ah , bh and δ as

$$\sigma_{II}(x) = \sigma_i \left(1 - \frac{x-ah}{bh-ah} \right) \quad (6)$$

where bh is the depth of tension zone, $0 \leq b \leq 1$.

At the equilibrium conditions of force and moment, following equations is satisfied

$$\int_0^{ah} \sigma_I(x) dx + \int_{ah}^h \sigma_{II}(x) dx = 0 \quad (7)$$

$$\int_0^{ah} \sigma_I(x)(h-x)B dx + \int_{ah}^h \sigma_{II}(x)(h-x)B dx = M \quad (8)$$

where M is the bending moment.

Eqs. (7) and (8) involve three unknown parameters a , b and δ . For a determination of these unknown parameters, it is assumed that the crack mouth opening, δ , can be expressed as (Zhang *et al.* 1999 and Tada 1985)

$$\delta = \frac{24a}{BhE} (MV_1(a) - M'V_2(a)) - \frac{4\sigma'ah}{E} V_3(a) \quad (9)$$

where, E is the Young's modulus of plain concrete.

$$M' = \int_0^{ah} B \sigma_I(x) \left(\frac{h}{2} - x \right) dx \quad (10)$$

$$\sigma' = \frac{1}{h} \int_0^{ah} \sigma_I(x) dx \quad (11)$$

$$V_1(a) = 0.33 - 1.42a + 3.87a^2 - 2.04a^3 + \frac{0.66}{(1-a)^2} \quad (12)$$

$$V_2(a) = 0.8 - 1.7a + 2.4a^2 + \frac{0.66}{(1-a)^2} \quad (13)$$

$$V_3(a) = \frac{1.46 + 3.42 \left(1 - \cos \frac{\pi a}{2} \right)}{\left(\cos \frac{\pi a}{2} \right)^2} \quad (14)$$

Numerical solution of the system of nonlinear Eqs. (7), (8) and (9) is applied to archive results of crack length, ah , and crack mouth opening, δ . In the first cycle, $\sigma_I(x)$ equals to σ_I according to Eq. (3) at $N=1$. In the second cycle, the stress degradation will occur in the cracked zone due to a

closing and opening procedure of fatigue crack. A new fictitious crack is needed so that the external load, P , can reach $P_{app, max}$ in the zone where fictitious crack has been formed already. Hence, the stress degradation law will be applied to both the old cracked zone and the newly developed crack zone, with $N = 2$ and $N = 1$, respectively. This procedure will be continued until σ_N equals to zero.

3. Prediction of chloride diffusion coefficient of cracked plain concrete under flexural cyclic load

Considering a simple case of chloride flow through cracked concrete, total flow of chloride can be expressed as the sum of the flow through crack and flow through uncracked part of homogeneous material, see Fig. 3. Thus, total flux of chloride through the entire cracked concrete can be written as follow (G erard and Marchand 2000)

$$J_{tot} = \frac{J_{ucr}A_{ucr} + J_{cr}A_{cr}}{A_{ucr} + A_{cr}} \tag{15}$$

where J_{tot} is the total flux of chloride through entire cracked concrete, mole/m²s. J_{ucr} is the flux of chloride through uncracked concrete, mole/m²s, and J_{cr} is the flux of chloride through cracks. A_{ucr} and A_{cr} , m², are the areas, which are perpendicular to the chloride flow, of cracks and uncracked concrete, respectively.

The flux of chloride can be expressed as multiplying the transport coefficient with the driving force, F .

$$J_{ucr} = -D_{ucr}F \tag{16}$$

$$J_{cr} = -D_{cr}F \tag{17}$$

$$J_{tot} = -D_{tot}F \tag{18}$$

where D_{ucr} and D_{cr} , m²/s, are the chloride diffusion coefficient of the uncracked concrete and through cracks, respectively. D_{tot} , m²/s, is the apparent chloride diffusion coefficient of the cracked concrete.

Replacing Eqs. (16), (17) and (18) into Eq. (15) gives:

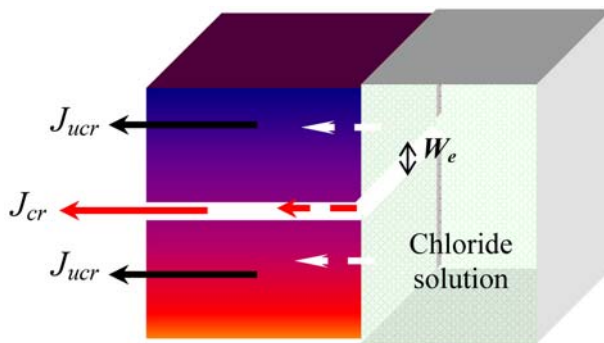


Fig. 3 The flux of chloride in cracked concrete

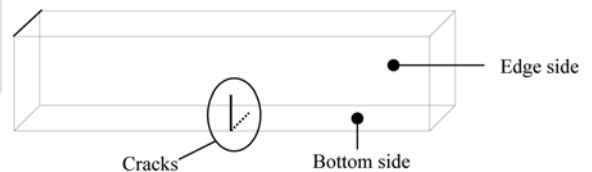


Fig. 4 Assumption of crack growth in concrete beam under flexural cyclic load

$$D_{tot} = \frac{A_{ucr}D_{ucr} + A_{cr}D_{cr}}{A_{ucr} + A_{cr}} \quad (19)$$

Kato *et al.* (2005) proposed that D_{cr} increases with increasing the crack width and becomes almost constant when the crack width is 0.075 mm or more. D_{cr} is approximately $2.51 \times 10^{-7} \text{ m}^2/\text{s}$ as the crack width is smaller than 0.075 mm.

For crack due to flexural cyclic load, we adopt the simple assumption that a single-edge crack occurs; the crack shape is straight; the crack length at the edge side is equal to that at the bottom side of the beam (Fig. 4). Hence, crack area, A_{cr} , can be expressed simply as

$$A_{cr} = W_e ah \quad (20)$$

where W_e , m , is the effective crack width. However, the actual crack due to flexural cyclic load is not simply straight, it is tortuous. In order to account for tortuous effect in an actual crack, W_e can be related to crack mouth opening δ and the tortuosity parameter, τ ($1 < \tau \leq 5$)

$$W_e = \frac{\delta}{\tau} \quad (21)$$

4. Numerical analysis and experimental verification of model

4.1 Mixture proportions and sample preparation

The concretes consist of Type I Portland cement, sand, crushed limestone aggregate with a maximum size of 20 mm and water. The concretes have water-cement ratios, w/c , of 0.4, 0.5 and 0.6. With each mixture, cylinder specimens, $\phi 100 \times 200$ mm, were prepared for the evaluation of the compression strength at 28 days. The concretes were cast in steel moulds and covered with plastic sheets after casting. The cylinder specimens were demoulded at one day of age and after that cured in lime saturated up to 28 day age. Concrete beams with dimensions of 400 mm in length, 100 mm in depth, and 100 mm in width, which were used for flexural cyclic test, were cast in two layers in steel moulds, covered by plastic sheets and also demoulded at the age of one day. Then, the prisms were cured in lime saturated for other 60 days for tests of flexural strength and flexural cyclic load. Mixing and casting were performed in the control room with temperature of $22 \pm 2^\circ\text{C}$ and relative humidity of $60 \pm 5\%$. The mixture proportions and properties of concretes are shown in Table 2.

4.2 Test of flexural cyclic load

The test of the flexural strength of concrete beam was conducted by ASTM C78 for determination of flexural ultimate load, P_{ult} . Then, the flexural cyclic test was performed with different load levels,

Table 2 Mixture proportions and properties of concrete

Series	w/c	Cement, kg/m^3	Water, kg/m^3	Coarse aggregate, kg/m^3	Sand, kg/m^3	σ_c , MPa	σ_b , MPa	E , GPa
M1	0.40	512	205	992	636	44	3.74	31.2
M2	0.50	410	205	992	738	37	3.33	28.6
M3	0.60	342	205	992	806	25	2.56	23.5

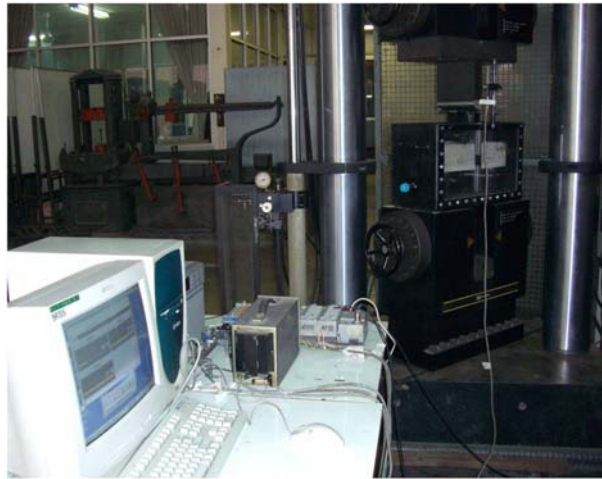


Fig. 5 Experimental set up and equipments used for tests of flexural cyclic load

Table 3 Flexural cyclic loads applied to concrete beams with different load levels

Series	P_{ult} , kN	SR			
		0.5	0.6	0.7	0.8
		$P_{app, max}$, kN			
M1	16	8.0	9.6	11.2	12.8
M2	15	7.5	9.0	10.5	12.0
M3	13	6.5	7.8	9.1	10.4

SR , which is ratio of maximum applied load, $P_{app, max}$, to ultimate load, P_{ult} . In the test of flexural cyclic load, Instron machine 1200 kN was used to apply third-point bending cyclic loads to concrete beams over span of 300 mm (Fig. 5). Deflection values of beams at middle bottom position were measured by LVDT. The load control test with low frequency of 0.01 Hz and load levels, SR , of 0.5, 0.6, 0.7 and 0.8 was used in this research. The load levels, SR , flexural ultimate load, P_{ult} , and maximum applied load, $P_{app, max}$, of different mixture series are shown in Table 3. Bending load was ramped up to the desired $P_{app, max}$ over about 20 cycles, then one-stage constant amplitude fatigue loading between $P_{app, max}$ and $P_{app, min}$, where $P_{app, min}$ equals to zero, was conducted. Based on curves of relationship of load and deflection shown in Fig. 6, in each load level, the specific number of cycles where the curves of relationship of load and deflection (herein after it is referred as to L-D curve) changed or not changed was determined. At cycles that L-D curve not changed and changed ($N = 2000, 2500, 3000, 3200, 3500$ and 3800), cubic specimens of 100 mm were taken from the middle bottom position of beams by sawing, see Fig. 7. Using these sawn specimens, crack widths of plain concrete in tension zone were measured by optical microscopy, and the chloride diffusion coefficients of plain concretes under different number of cycles and load levels were determined. A modified chloride migration test, which combines ASTM C1202 and NTBUILD 492, was applied for determination of the chloride diffusion coefficient. This modified test uses cubic specimens with a dimension of 100 mm and a thickness of 50 mm. The specimens were placed in two chambers: a chamber with 3% sodium chloride and the other chamber with 0.3N sodium hydroxide, and an

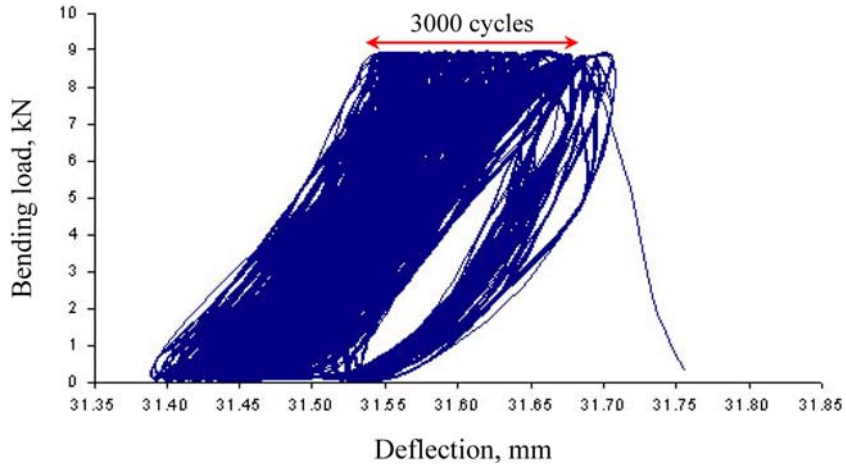


Fig. 6 Typical destructive flexural fatigue results for a load control test, $SR = 0.7$

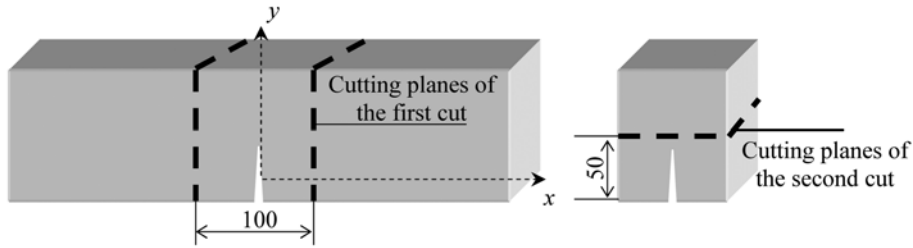


Fig. 7 Schematic representation of cutting planes

external electrical potential of 30V was applied axially across the specimen to force the chloride ions outside to migrate into the specimen. After 12 hours of testing duration, the specimen was split axially and a silver nitrate solution sprayed onto one of the freshly split sections. The chloride penetration depth could then be measured from the visible white silver chloride precipitation. The chloride diffusion coefficient was calculated from this penetration depth through Eq. (22). The detail of this test can refer to (NORDTEST 1999 and Tran *et al.* 2009).

$$D = \frac{0.0239(273+T)L}{(U-2)t} \left(x_d - 0.0238 \sqrt{\frac{(273+T)Lx_d}{U-2}} \right) \quad (22)$$

where D is chloride diffusion coefficient, m^2/s , U is absolute value of the applied voltage, V , T is average value of the initial and final temperatures, $^{\circ}C$, L is thickness of the specimen, mm , x_d is average value of the penetration, mm , t is test duration, hour.

4.3 Fatigue crack width and crack length

In the fatigue test under load control procedure, bending load was ramped up to the desired $P_{app, max}$ over 20 cycles, the elastic displacement at this desired $P_{app, max}$, with $SR = 0.7$, was about 0.01 mm (Gontar *et al.* 2000). So, the numerical analyses of the fatigue deformation adopt 0.007, 0.008, 0.01 and 0.011 mm as the initially ramped up crack width, w_b , these fatigue deformations are corresponding to SR of 0.5, 0.6, 0.7 and 0.8, respectively. Numerical analyses of relationships between crack width

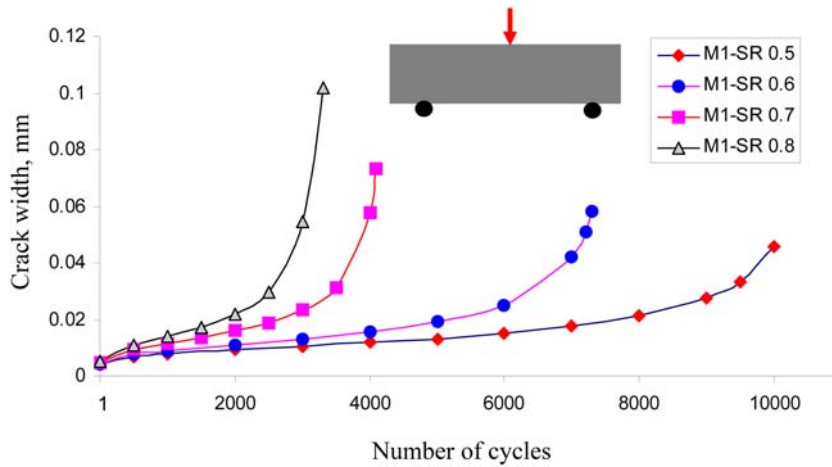


Fig. 8 Predictions of relationships of crack width and number of cycles

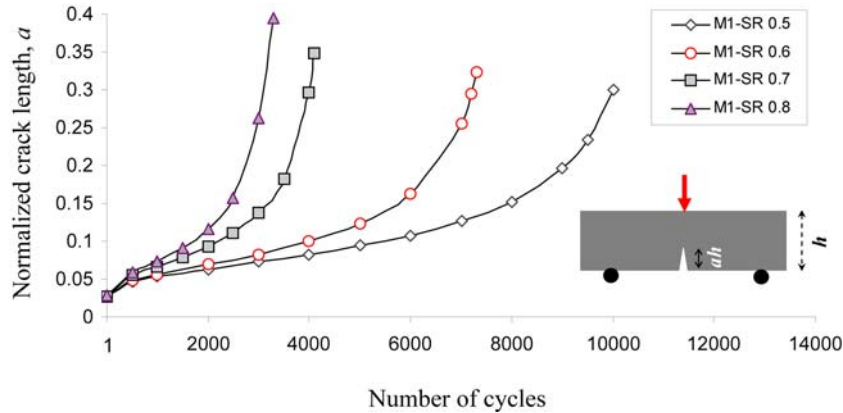


Fig. 9 Predictions of relationships of crack length and number of cycles

and the number of cycles for plain concrete beam subjected to fatigue tests with different SR are shown in Fig. 8. The theoretically calculated fatigue crack lengths of concrete beams under different load levels with the minimum applied load, $P_{app,min}$, equal to zero are shown in Fig. 9. The fictitious crack width and crack length increased with increasing either the number of cycles or the load level, SR . The numerical simulation clearly showed that fictitious crack growth, in terms of crack width and crack length, can be divided into three stages; a decelerated stage; a steady stage; an accelerated stage towards fracture. These results are consistent with other reports (Zhang *et al.* 1999 and Ulfkjær *et al.* 1995), and with experimental data shown in Fig. 6. However, as shown in Fig. 10, the numerical results of crack widths do not fit well with experimental data obtained by optical microscopy. One reason for this is that the fatigue load may cause multiple microcracks in concrete than results of the numerical prediction with a single crack. Indeed, the numerical predicted crack width is larger than the measured crack width. Good fitting between the model estimation and experimental data is found when the authors introduce a so-called crack density parameter, μ , which takes into account microcracks beside the main crack. μ is a function of the number of cycles, N , and load level, SR , as below:

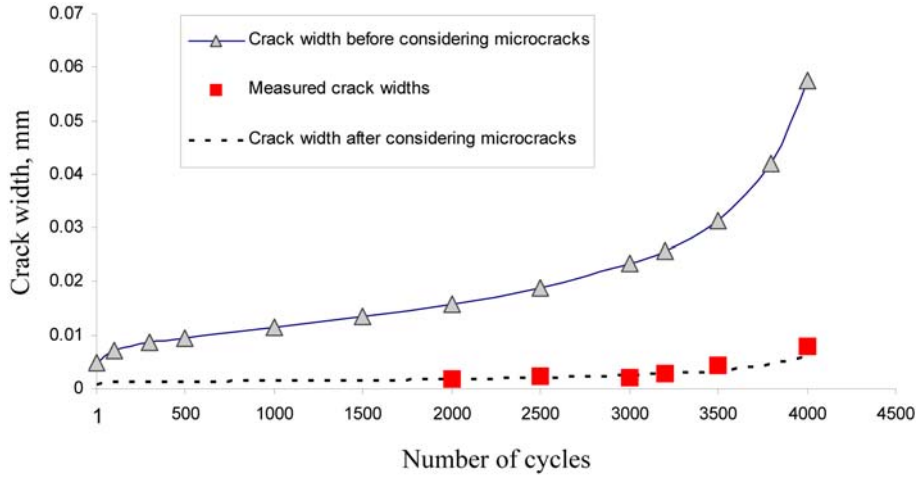


Fig. 10 Relationships of crack width and number of cycles, model prediction and experimental results, M1, $SR = 0.7$

$$\mu = \left(\frac{1}{SR}\right)^2 \log(N) + 2.2 \tag{23}$$

4.4 Chloride diffusion coefficient under fatigue

Model prediction on the effect of the number of cycles on the chloride diffusion, normalized D_{tot} , in the tension zone of plain concrete beams, which are under the flexural cyclic load, is shown in Fig. 11. Table 4 shows the model results of the calculated chloride diffusion coefficient in the tension zone with the number of cycles. Fig. 11 and Table 4 clearly show that the chloride diffusion in the tension zone increases with the number of cycles. Although microcracks are decelerated with the number of cycles from 0 to 500, when load level SR was 0.7, as shown in Figs. 8, 9 and 10, the

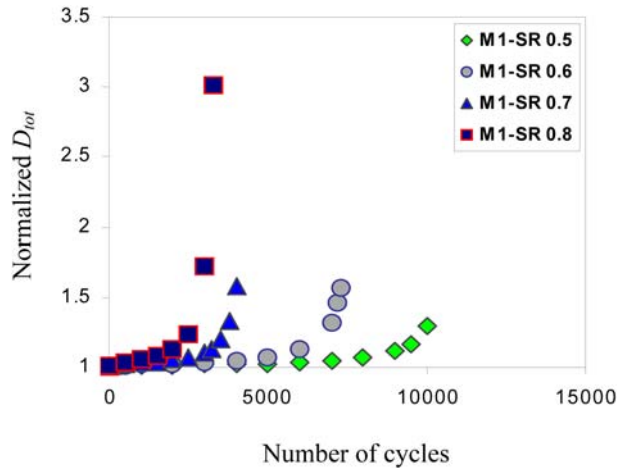


Fig. 11 Model prediction for the chloride diffusion coefficient in tension zone of plain concrete beam with the number of cycles and load levels, M1

Table 4 Values of D_{tot} of plain concrete in the tension zone with the number of cycles

Series	SR	$D_{tot} \times 10^{-12} \text{ m}^2/\text{s} (N)$													
M1	0.5	6.25 (0)	6.29 (1)	6.31 (500)	6.32 (1000)	6.34 (2000)	6.37 (3000)	6.39 (4000)	6.43 (5000)	6.48 (6000)	6.56 (7000)	6.70 (8000)	6.99 (9000)	7.31 (9500)	8.10 (10000)
	0.6	6.25 (0)	6.30 (1)	6.34 (500)	6.37 (1000)	6.41 (2000)	6.47 (3000)	6.56 (4000)	6.71 (5000)	7.03 (6000)	8.29 (7000)	9.11 (7200)	9.81 (7300)	-	-
	0.7	6.25 (0)	6.29 (1)	6.35 (100)	6.37 (300)	6.39 (500)	6.45 (1000)	6.51 (1500)	6.61 (2000)	6.74 (2500)	6.98 (3000)	7.14 (3200)	7.54 (3500)	8.45 (3800)	10.06 (4000)
	0.8	6.25 (0)	6.31 (1)	6.49 (500)	6.61 (1000)	6.78 (1500)	7.07 (2000)	7.74 (2500)	10.80 (3000)	18.90 (3300)	-	-	-	-	-
M2	0.5	13.10 (0)	13.10 (1)	13.20 (500)	13.20 (1000)	13.20 (2000)	13.20 (3000)	13.20 (4000)	13.30 (5000)	13.30 (6000)	13.40 (7000)	13.60 (8000)	13.80 (9000)	14.20 (9500)	15.0 (10000)
	0.6	13.10 (0)	13.10 (1)	13.20 (500)	13.20 (1000)	13.30 (2000)	13.30 (3000)	13.40 (4000)	13.60 (5000)	13.90 (6000)	15.20 (7000)	16.10 (7200)	16.80 (7300)	-	-
	0.7	13.10 (0)	13.20 (1)	13.30 (500)	13.30 (1000)	13.40 (1500)	13.50 (2000)	13.70 (2500)	14.00 (3000)	14.60 (3500)	17.60 (4000)	19.90 (4100)	-	-	-
	0.8	13.10 (0)	13.20 (1)	13.30 (500)	13.50 (1000)	13.60 (1500)	13.90 (2000)	14.60 (2500)	17.80 (3000)	26.40 (3200)	-	-	-	-	-
M3	0.5	15.90 (0)	15.90 (1)	16.00 (500)	16.00 (1000)	16.00 (2000)	16.00 (3000)	16.10 (4000)	16.10 (5000)	16.10 (6000)	16.20 (7000)	16.40 (8000)	16.70 (9000)	17.10 (9500)	17.90 (10000)
	0.6	15.90 (0)	16.00 (1)	16.00 (500)	16.00 (1000)	16.10 (2000)	16.10 (3000)	16.20 (4000)	16.40 (5000)	16.80 (6000)	18.20 (7000)	19.10 (7200)	19.90 (7300)	-	-
	0.7	15.90 (0)	16.00 (1)	16.10 (500)	16.10 (1000)	16.20 (1500)	16.30 (2000)	16.50 (2500)	16.80 (3000)	17.50 (3500)	20.80 (4000)	23.40 (4100)	-	-	-

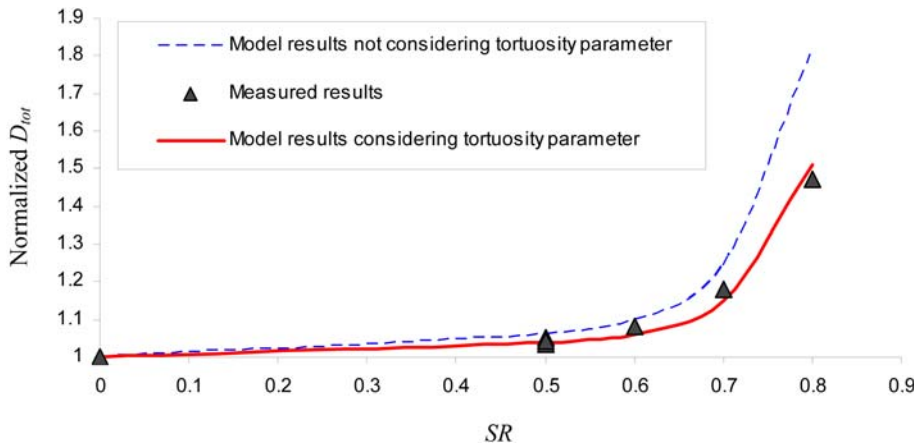


Fig. 12 Relationships of load level and normalized D_{tot} , model prediction and experimental results, M1, $N = 3000$

chloride diffusion still seems to be monotonously increasing (Fig. 11). One of the reasons is that decelerated microcracks are still so small that crack areas formed are still not large enough, compared to the whole surface area of the specimen, to change the chloride diffusion readily. Thus, with $SR = 0.7$, overall, when the fatigue load was applied up to the number of cycles of 3000, the

chloride diffusion is monotonously increasing. However, from 3000 cycles, crack widths start to enhance up to the failure, which results in large crack areas corresponding with a so-called accelerated stage of the chloride diffusion. In this stage, cracks may not be able to heal in unloaded stage, or cracks become irreversible to contribute for widening accesses for the chloride diffusion.

The effect of fatigue load level on the chloride diffusion coefficient in tension zone is shown in Fig. 12. As can be seen in Fig. 12, with the same mixture series and the same number of cycle, the experiments show an increasing tendency of the chloride diffusion with increasing the load level. The chloride diffusion increases significantly when we apply fatigue test with load level SR at 0.6, 0.7 and 0.8, especially at 0.7 and 0.8. The model prediction shows the same tendency of the chloride diffusion with measurements. However, at any the load level of fatigue test, the normalized D_{tot} (against the control without fatigue test, $SR = 0$) predicted by the model is always higher than that measured by the experiment. A main reason is that we use the assumption of the singly straight crack developed with the number of cycles. Practically, with the number of cycles, the crack is tortuous and the width of the crack along the path varies significantly. When we introduce tortuosity parameter, τ , with $\tau = 1.65$, to account for the intrinsic tortuosity of the crack, good agreement between model predictions and measured results, simulated crack width after considering the crack density divided by τ , can be found.

5. Conclusions

- An analytical approach for modeling the influence of flexural cyclic load on the chloride diffusion coefficient in the tension zone of plain concrete that depends on the stress degradation law and the steady-state transport of chloride ions as the fundamental assumptions was presented. When we introduced the crack density parameter, μ , and the tortuosity parameter, τ , the model predictions fit well with experimental results.
- In this model, three cracking stages are described. However, two stages of increasing the chloride diffusion coefficient in the tension zone are represented including the monotonous increase and the accelerated increase.
- Under flexural cyclic load, the non-linear relationship between load level, SR , and the chloride diffusion coefficient in the tension zone of plain concrete is found both in model predictions and experiments. Model predictions show an increasing tendency of the chloride diffusion coefficient with increasing load level, SR , especially at $SR = 0.7$ and 0.8 .

Acknowledgements

The authors gratefully acknowledge Japan International Cooperation Agency (JICA) for supporting to this research through AUN/SEED-Net Program.

References

- Byung, B. and Oh, H. (1986), "Fatigue analysis of plain concrete in flexure", *J. Struct. Eng.*, **112**(2), 273-288.
Chapra, S.C. and Canale, R.P. (1998), *Numerical methods for engineers*, Second Edition, McGraw-Hill.

- Crank, J. (1975), *The mathematics of diffusion*, Oxford Press.
- Gontar, W.A., Martin, J.P. and Popovics, J.S. (2000), "Effects of cyclic loading on chloride permeability of plain concrete", *Proceeding of ASCE International Conference of Condition monitoring of Materials and Structures*, Austin-Texas.
- Gowripalan, N., Sirivivatnanon, V. and Lim, C.C. (2000), "Chloride diffusivity of concrete cracked in flexure", *Cement Concrete Res.*, **30**(5), 725-730.
- Gérard, B. and Marchand, J. (2000), "Influence of cracking on the diffusion properties of cement-based materials, Part I: Influence of continuous cracks on the steady-state regime", *Cement Concrete Res.*, **30**(1), 37-43.
- Kato, E., Kato, Y. and Uomoto, T. (2005), "Development of simulation model of chloride ion transportation in cracked concrete", *J. Adv. Concrete Tech.*, **3**(1), 85-94.
- NORDTEST (1999), *Concrete, mortar and cement-based repair materials: chloride migration coefficient from non-steady-state migration experiments*, Nordisk InnovationsCenter, Finland.
- Scheidegger, A.E. (1974), *The physics of flow through porous media*, University of Toronto Press.
- Tada, H. (1985), *The stress analysis of cracks handbooks*, Paris Prod. Inc.
- Tralla, J.P. and Silfwerbrand, J. (2002), "Estimation of chloride ingress in uncracked and cracked concrete using measured surface concentrations", *ACI Mater. J.*, **99**(1), 27-36.
- Tran, M.V., Stitmannathum, B. and Nawa, T. (2009), "Simulation of chloride penetration into concrete structures subjected to both flexural cyclic loads and tidal effects", *Comput. Concrete*, **6**(5), 421-435.
- Ulfkjær, J.P., Krenk, S. and Brincker, R. (1995), "Analytical model for fictitious crack propagation in concrete beams", *J. Eng. Mech.*, **121**(1), 7-14.
- Yoon, I.S. (2009), "Simple approach to calculate chloride diffusivity of concrete considering carbonation", *Comput. Concrete*, **6**(1), 1-18.
- Zhang Jun, Stang, Henrick and Victor, C.L. (1999), "Fatigue life prediction of fiber reinforced concrete under flexural load", *Int. J. Fatigue*, **21**(10), 1033-1049.